3

Structural and Optical Behavior of Vanadate-Tellurate Glasses Containing PbO or Sm_2O_3

E. Culea[1], S. Rada[1], M. Culea[2] and M. Rada[3]
[1]*Department of Physics and Chemistry, Technical University of Cluj-Napoca, Cluj-Napoca*
[2]*Faculty of Physics, Babes-Bolyai University of Cluj-Napoca, Cluj-Napoca*
[3]*National Institute for R&D of Isotopic and Molecular Technologies, Cluj-Napoca*
Romania

1. Introduction

Tellurium oxide based glasses are of scientific and technological interest due to their unique properties such as chemical durability, electrical conductivity, transmission capability, high refractive indices, high dielectric constant and low melting points [1-3].

Tellurate glasses have recently gained wide attention because of their potential as hosts of rare earth elements for the development of fibres and lasers covering all the main telecommunication bands and promising materials for optical switching devices [4, 5]. Recently, tellurate glasses doped with heavy metal oxides or rare earth oxides have received great scientific interest because these oxides can change the optical and physical properties of the tellurate glasses [5].

Vanadium tellurate glasses showed better mechanical and electrical properties due to the V_2O_5 incorporated into the tellurate glass matrix. In the case of V_2O_5 contents below 20mol%, the three-dimensional tellurate network is partially broken by the formation of [TeO_3] trigonal pyramidal units, which in turn reduce the glass rigidity and. When the V_2O_5 concentration is above 20mol%, the glass structure changes from the continuous tellurate network to the continuous vanadate network [6].

Due to the large atomic mass and high polarizability of the Pb^{+2} ions, heavy metal oxide glasses with PbO possess high refractive index, wide infrared transmittance, and hence they are considered to be promising glass hosts for photonic devices [7, 8]. The special significance of PbO is that it contributes to form stable glasses over a wide range of concentrations due to its dual role as glass modifier and glass former.

Rare-earth ions doped glasses have been prepared and characterized to understand their commercial applications as glass lasers and also in the production of wide variety of other types of optical components [9].

The luminescence spectral properties of rare earth ions such as Eu^{+3} ($4f^6$) and Tb^{+3} ($4f^8$), Sm^{+3} ($4f^5$) and Dy^{+3} ($4f^9$) in the heavy-metal borate glasses have shown interesting and encouraging results [10, 11]. Eu^{+3} and Tb^{+3} ions have shown prominent emissions (red and green) in the visible wavelength region, while Sm^{+3} and Dy^{+3} show strong absorption bands

in the NIR range (800–2200 nm) and intense emission bands in the visible region (550–730 nm) [11].

The present work deals with the role of lead and samarium ions in the short-range structural order of the vanadate-tellurate glass network. Lead and samarium-activated vanadate-tellurate glasses have been investigated using infrared spectroscopy and ultraviolet-visible spectroscopy. The main goal is to obtain information about the influence of the radii and concentration of lead and samarium ions on the TeO_4/TeO_3 and VO_5/VO_4 conversion in vanadate-tellurate glasses and especially to illuminate aspects of the vanadate glass network using DFT calculations.

2. Experimental procedure

Glasses were prepared by mixing and melting of appropriate amounts of lead (IV) oxide, tellurium oxide (IV), lead (II) oxide or samarium (III) oxide of high purity (99,99%, Aldrich Chemical Co.). Reagents were melted at 875^0C for 10minutes and quenched by pouring the melts on stainless steel plates.

The samples were analyzed by means of X-ray diffraction using a XRD-6000 Shimadzu diffractometer, with a monochromator of graphite for the Cu-Kα radiation (λ=1.54Å) at room temperature.

The FT-IR absorption spectra of the glasses in the 370-1100cm^{-1} spectral range were obtained with a JASCO FTIR 6200 spectrometer using the standard KBr pellet disc technique. The spectra were carried out with a standard resolution of 2cm^{-1}.

UV-Visible absorption spectra measurements in the wavelength range of 250-1050nm were performed at room temperature using a Perkin-Elmer Lambda 45 UV/VIS spectrometer equipped with an integrating sphere. These measurements were made on glass powder dispersed in KBr pellets. The optical absorption coefficient, α, was calculated from the absorbance, A, using the equation:

$$\alpha = 2.303\ A/d$$

where d is the thickness of the sample.

The starting structures have been built using the graphical interface of Spartan'04 [12] and preoptimized by molecular mechanics. Optimizations were continued at DFT level (B3LYP/CEP-4G/ECP) using the Gaussian'03 package of programs [13].

It should be noticed that only the broken bonds at the model boundary were terminated by hydrogen atoms. The positions of boundary atoms were frozen during the calculation and the coordinates of internal atoms were optimized in order to model the active fragment flexibility and its incorporation into the bulk.

3. Results and discussion

The vitreous or/and crystalline nature of the $xPbO\cdot(100\text{-}x)(3TeO_2\cdot 2V_2O_5)$ and $xSm_2O_3\cdot(100\text{-}x)(3TeO_2\cdot 2V_2O_5)$ samples with various contents of lead or samarium oxide ($0\leq x\leq 50$mol%) was tested by X-ray diffraction. The X-ray diffraction patterns of the studied samples are shown in Fig. 1. The X-ray diffraction patterns did not reveal the crystalline phases in the

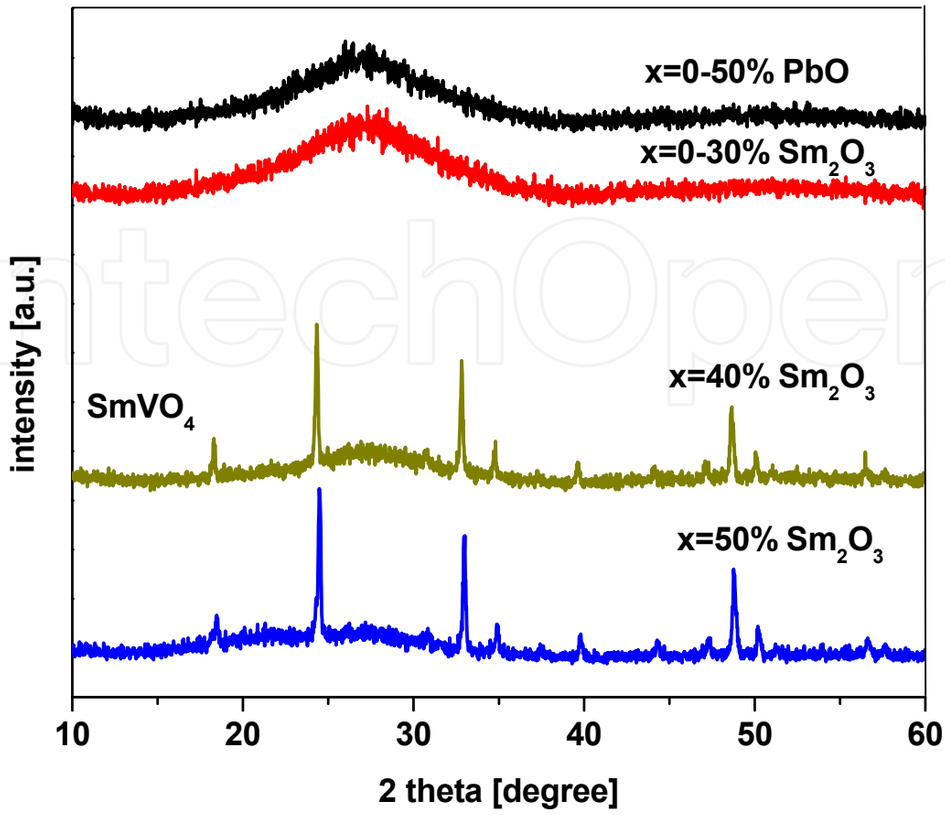

Fig. 1. X-ray diffraction patterns for xPbO (or xSm_2O_3)·(100-x)[$3TeO_2$·$2V_2O_5$] samples where 0≤x≤50mol%.

samples with 0≤x≤50mol% PbO while in the samples with x≥40mol% Sm_2O_3 the presence of the SmVO4 crystalline phase was detected.

3.1 FTIR spectroscopy

The absorption bands located around 460cm^{-1}, 610-680 and 720 to 780cm^{-1} are assigned to the bending mode of Te-O-Te or O-Te-O linkages, the stretching mode of [TeO_4] trigonal pyramids with bridging oxygen and the stretching mode of [TeO_3] trigonal pyramids with non-bridging oxygen, respectively [14-18].

The IR spectrum of the pure crystalline and amorphous V_2O_5 is characterized by the intense band in the 1000-1020cm^{-1} range which is related to vibrations of isolated V=O vanadyl groups in [VO_5] trigonal bipyramids. The band located at 950-970cm^{-1} was attributed to the [VO_4] units [19-21].

The examination of the FTIR spectra of the xM_aO_b·(100-x)[$3TeO_2$·$2V_2O_5$] where M_aO_b = PbO or Sm_2O_3 glasses and glass ceramics shows some changes in the characteristic bands corresponding to the structural units of the glass network (Fig. 2). These modifications can be summarized as follows:

1. x =10mol% M_aO_b (1)

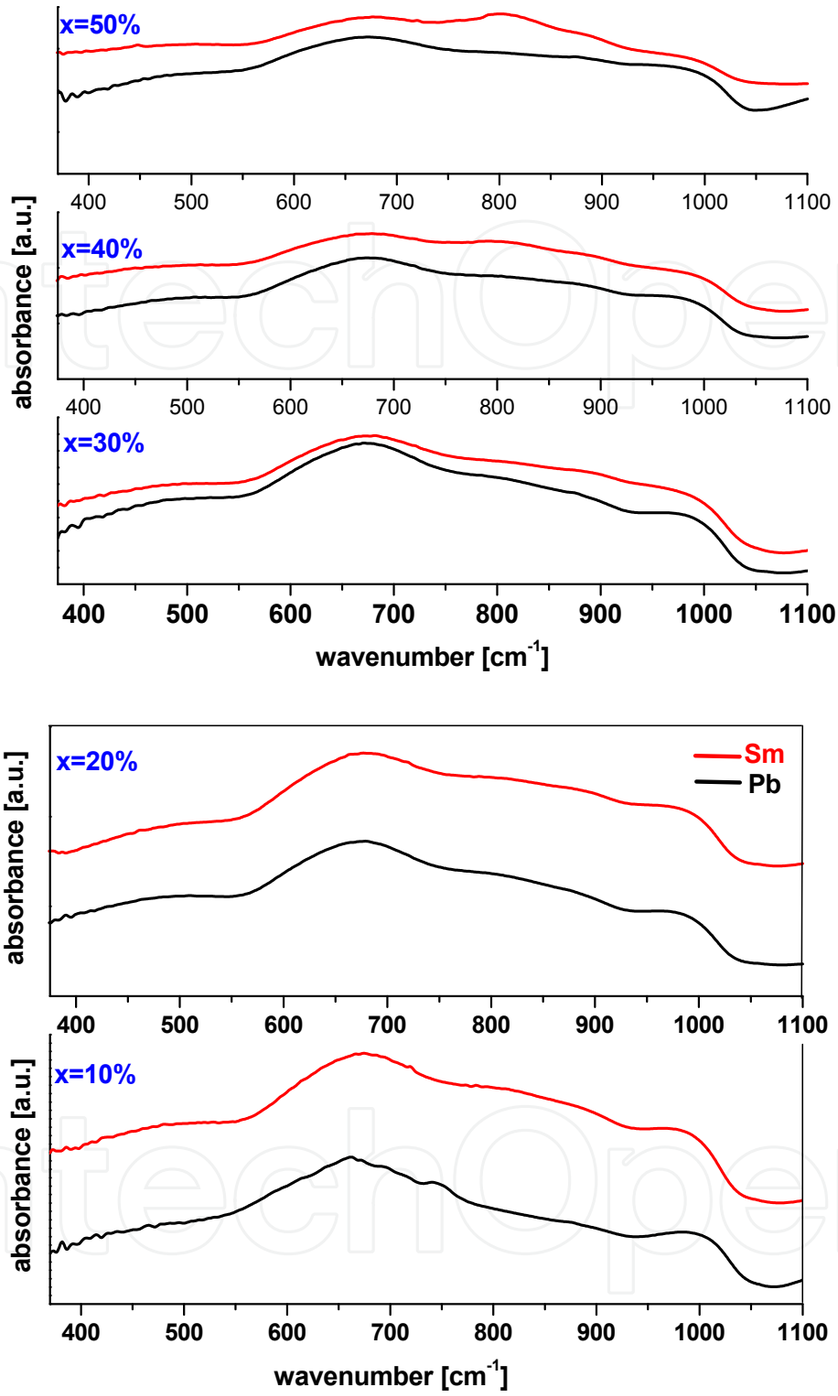

Fig. 2. FTIR spectra of xPbO (or xSm_2O_3)·(100-x)[$3TeO_2$·$2V_2O_5$] samples where 0≤x≤50mol%.

The incorporation of network modifier lead ions into the vanadate-tellurate glasses enhances the breaking of axial Te-O-Te linkages in the [TeO_4] trigonal bypiramidal structural units. As a consequence, three-coordination tellurium is formed and accumulated. The band centered at about 750cm^{-1} indicates the presence of the [TeO_3] structural units [17,

18]. The [TeO_3] structural units are expected to participate in the depolymerization of the glass network because they create more bonding defects and non-bonding oxygens.

The intensity of the band corresponding to the [TeO_3] units (located at about ~750cm^{-1}) decreases and a new band located at about 800cm^{-1} appears with the adding of the Sm_2O_3 content. In detail, the band situated at about 800cm^{-1} is due to the asymmetric stretching of VO_4^{-3} entity from orthovanadate species [22, 23].

2. $10 \leq x \leq 30$ mol% M_aO_b (2)

An increasing trend was observed in the strength of the bands centered at ~1020cm^{-1}. The feature of the band located at about 875cm^{-1} comes up in intensity. This effect is more pronounced when adding of samarium ions in the matrix network. This band is attributed to the vibrations of the V-O bonds from the pyrovanadate structural units.

The gradual addition of the samarium (III) oxide leads not only to a simple incorporation of these ions in the host glass matrix but also generates changes of the basic structural units of the glass matrix. Structural changes reveal that the samarium ions causes a change from the continuous vanadate-tellurate network to a continuous samarium-vanadate-tellurate network interconnected through Sm-O-V and Te-O-Sm bridges. Then, the surplus of non-bridging oxygens is be converted to bridging ones leading to the decrease of the connectivity of the network.

3. $x \geq 40$mol% M_aO_b (3)

By increasing the Sm_2O_3 content up to 40mol%, the evolution of the structure can be explained considering the higher capacity of migration of the samarium ions inside the glass network and the formation of the $SmVO_4$ crystalline phase, in agreement with XRD data. The accumulation of oxygen atoms in the glass network can be supported by the formation of ortho- and pyro-vanadate structural units.

On the other hand, the lead oxide generates the rapid deformation of the Te-O-Te linkages yielding the formation of [TeO_3] structural units. Further, the excess of oxygen can be accommodated in the host matrix by conversion of some [VO_4] structural units into [VO_5] structural units.

The broader band centered at ~ 670-850cm^{-1} can be attributed to the Pb-O bonds vibrations from the [PbO4] and [PbO3] structural units. The absorption band centered at about 470cm^{-1} may be correlated with the Pb-O stretching vibration in [PbO_4] structural units [24-26]. The increase in the intensity of the bands situated between 650 and 850cm^{-1} show that the excess of oxygen in the glass network can be supported by the increase of [PbO_n] structural units (with n=3 and 4).

In brief, the variations observed in the FTIR spectra suggest a gradual inclusion of the lead ions in the host vitreous matrix with increasing of the PbO content up to 50mol%, while progressive adding of samarium oxide determines the increase in the intensity of the bands due to the ortho- and pyrovanadate structural units. The mechanisms of incorporation of the lead and samarium ions in the host matrices can be summarized as following:

i. For the samples with lead oxide, the Pb^{+2} ions can occupy a position in the chain itself and their influence on the V=O bonds is limited. Since the V=O mode position from about 1020cm^{-1} is preserved it can be concluded that the V=O bond is not directly influenced and the coordination number and symmetry of the [VO_4] and [VO_5] structural units do not change significantly. The increase in the intensity of the bands situated at 650 and 850cm^{-1} show that the PbO acts as a network former with a moderate effect on the vanadate-tellurate network.
ii. By increasing the samarium oxide content up to 30mol%, Sm^{+3} ions located between the vanadate chains may affect the isolated V=O bonds yielding to the depolimerization of the vanadate network in shorter and isolated chains formed of ortho- and pyro-vanadate structural units. As a result they are markedly elongated and the vibrations frequency shifts toward lower wavenumbers. The increase of the content of samarium ions produces a strong depolymerization of the network leading to formation of $SmVO_4$ crystalline phase, in agreement with the XRD data. The combined XRD and IR spectroscopy data show that the Sm_2O_3 acts as a network modifier with a strong effect about vanadate network.

3.2 UV-VIS spectroscopy

Optical absorption in solids occurs by various mechanisms, in all of which the phonon energy will be absorbed by either the lattice or by electrons where the transferred energy is covered. The lattice (or phonon) absorption will give information about atomic vibrations involved and this absorption of radiation normally occurs in the infrared region of the spectrum. Optical absorption is a useful method for investigating optically induced transitions and getting information about the energy gap of non-crystalline materials and the band structure. The principle of this technique is that a photon with energy greater than the band gap energy will be absorbed [27].

One of the most important concerns in rare earth doped glasses is to define the dopant environment. Hypersensitive transitions are observed in the spectra of all rare earth ions having more than one f electrons. Hypersensitive transitions of rare earth ions manifest an anomalous sensitivity of line strength to the character of the dopant environment [28, 29].

The measured UV-VIS absorption spectra of the lead and samarium-vanadate-tellurate glasses are shown in Fig. 3. The spectra show that the maxima of the absorption are located in the UV region for all investigated glasses containing PbO or Sm_2O_3.

The Pb^{+2} ions absorb strongly in the ultraviolet (310nm) and yield broad emission bands in the ultraviolet and blue spectral area [30]. The Sm^{+3} ions have five electrons in the f shell. The absorption bands due to the electron jump from the $^6H_{5/2}$ ground state to the $^6P_{5/2}$ (365nm), $^6P_{7/2}$ (375nm), $^6P_{3/2}$ (400nm), $^4K_{11/2}$ (415nm), $^4F_{15/2}$ (460nm) and $^4F_{13/2}$ (475nm) excited states were observed [31].

The stronger transitions in the UV region can be due to the presence of the Te=O bonds from the [TeO_3] structural units, the Pb=O bonds from [PbO_3] structural units and the V=O bonds from [VO_4] structural units which allow n-π^* transitions. The intensity of these bands slightly increases and shifts towards higher wavelengths with increasing the concentration of PbO and Sm_2O_3. This may be due to the increase of the number of the V=O bonds from

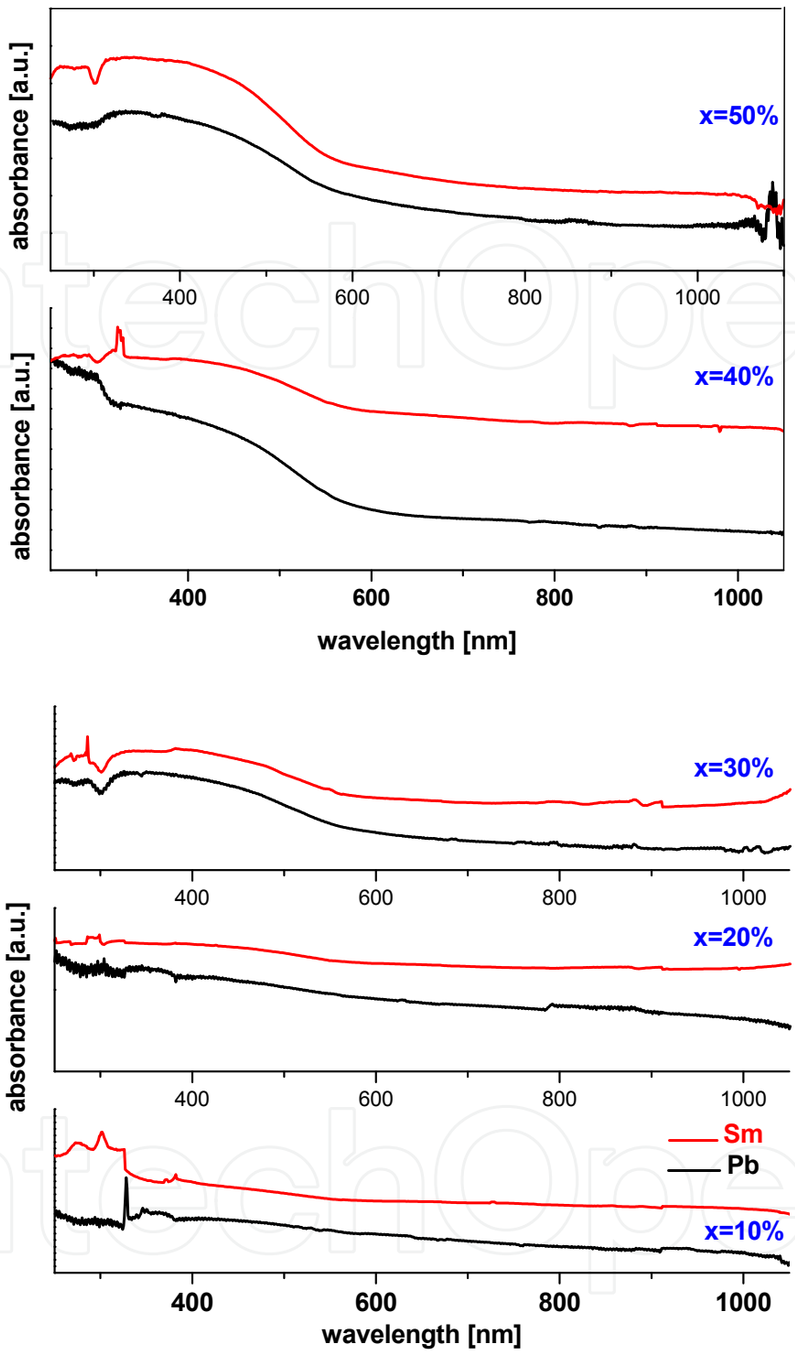

Fig. 3. UV-VIS absorption spectra of $xPbO$ (or xSm_2O_3)·(100-x)[$3TeO_2$·$2V_2O_5$] samples where 0≤x≤50mol% in function of lead (II) or samarium (III) oxide content.

orthovanadate structural units for the samples with Sm_2O_3 content and the increase of the number of [PbO_3] structural units in the samples with PbO.

The measurements of optical absorption and the absorption edge are important especially in connection with the theory of electronic structure of amorphous materials. The energy gap,

Eg, is an important feature of semiconductors which determines their applications in optoelectronics [32]. Observations of the variation of E_g with increase in the modifier content can be attributed to the changes in the bonding that takes place in the glass

The nature of the optical transition involved in the network can be determined on the basis of the dependence of absorption coefficient (α) on phonon energy (hυ). The total absorption could be due to the optical transition which is fitted to the relation:

$$\alpha\, h\upsilon = \alpha_0 (h\upsilon - Eg)^n$$

where E_g is the optical energy gap between the bottom of the conduction band and the top of the valence band at the same value of wavenumber, α_0 is a constant related to the extent of the band tailing and the exponent n is an index which can have any values between ½ and 2 depending on the nature of the interband electronic transitions.

Extrapolating the linear portion of the graph $(\alpha h\nu)^2 \rightarrow 0$ to hν axis, the optical band gaps, E_g are determined with increasing PbO and Sm_2O_3 content (Figs. 4 and 5). The optical band gap increases gradually from 1.84eV to 2.09eV and 2.21eV, respectively, by adding of PbO and Sm_2O_3. In either case the values are systematically increasing with the increase of x. It is to be noted that the curves are characterized by the presence of an exponential decay tail at low energy. These results indicate the presence of a well defined $\pi \rightarrow \pi^*$ transition associated with the formation of conjugated electronic structure [33].

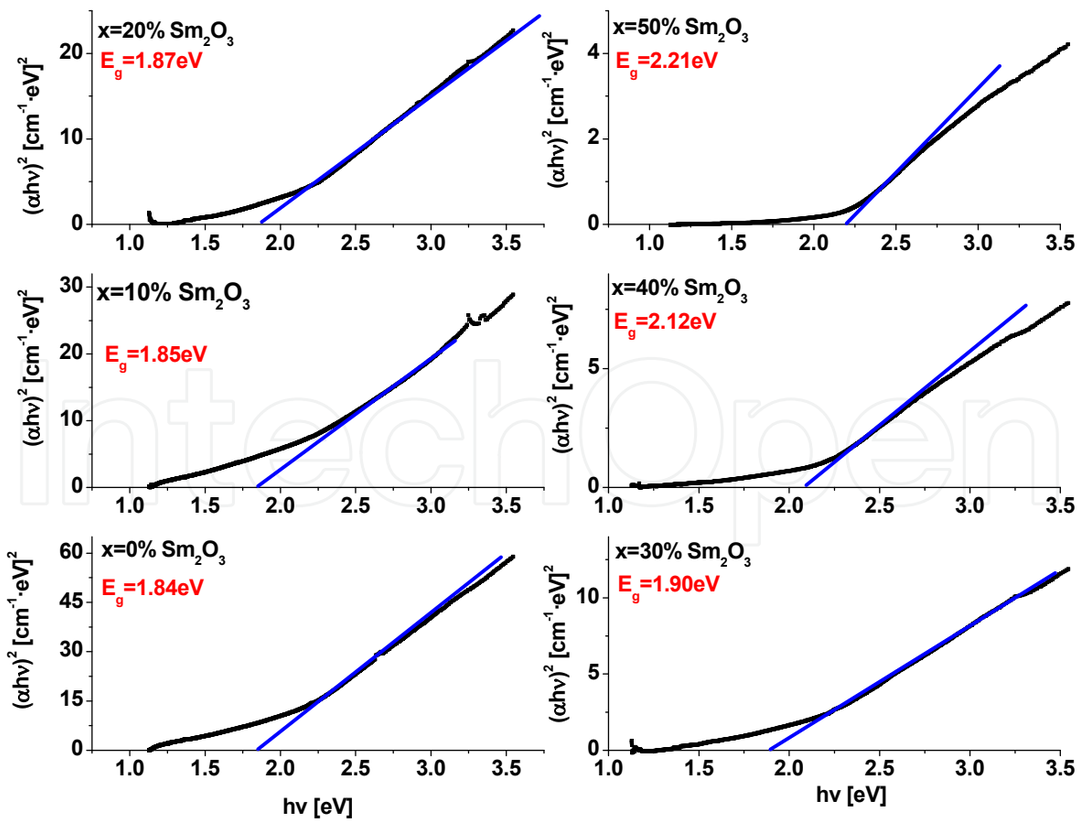

Fig. 4. Plots of $(\alpha h\nu)^2$ versus hν for $xPbO\cdot(100\text{-}x)[3TeO_2\cdot 2V_2O_5]$ glasses where 0≤x≤50mol%

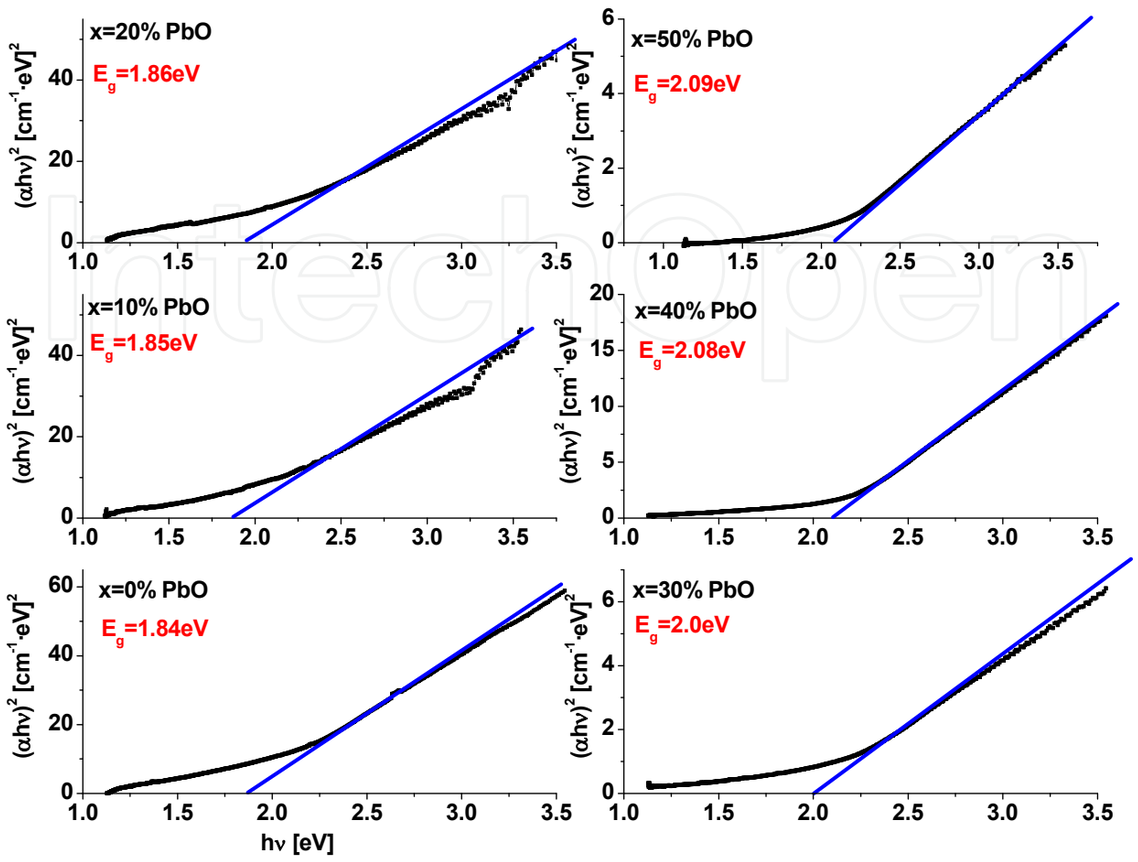

Fig. 5. Plots of $(\alpha h\nu)^2$ versus hν for $xSm_2O_3 \cdot (100-x)[3TeO_2 \cdot 2V_2O_5]$ samples where $0 \leq x \leq 50$mol%.

The increase of the band gap may occur due to variation in non-bridging oxygen ion concentrations. In metal oxides, the valence band maximum mainly consists of 2p orbital of the oxygen atom and the conduction band minimum mainly consists of ns orbital of the metal atom. The non-bridging oxygen ions contribute to the valence band maximum. The non-bridging orbitals have higher energies than bonding orbitals. When a metal-oxygen bond is broken, the bond energy is released. The increase in concentration of the non-bridging oxygen ions results in the shift of the valence band maximum to higher energies and the reduction of the band gap. Thus, the enlarging of band gap energy due to increase in the PbO or Sm_2O_3 content suggests that non-bridging oxygen ion concentration decreases with increasing the PbO or Sm_2O_3 content that expands the band gap energy. In the glasses doped with Sm_2O_3, the non-bridging oxygen ions concentration decreases due to the formation of orthovanadate structural units. In the glasses doped with PbO, the non-bridging oxygen ions concentration decreases also because the lead atoms act as network formers and the accommodation with the excess of oxygen ions is possible by the increase of the polymerization degree of the network by Pb-O-Te and Pb-O-V linkages.

The existence and variation of optical energy gap may be also explained by invoking the occurrence of local cross linking within the amorphous phase of the matrix network, in such a way as to increase the degree of ordering in these parts.

Refractive index is one of the most important properties in optical glasses. A large number of researchers have carried out investigations to ascertain the relation between refractive index and glass composition. It is generally recognized that the refractive index, n, of many common glasses can be varied by changing the base glass composition [34].

The observed decrease in the refractive index of the studied glasses accompanying to the addition of PbO or Sm_2O_3 content presented in the Fig. 6 can be considered as an indication of a decrease in number of non-bridging oxygen ions.

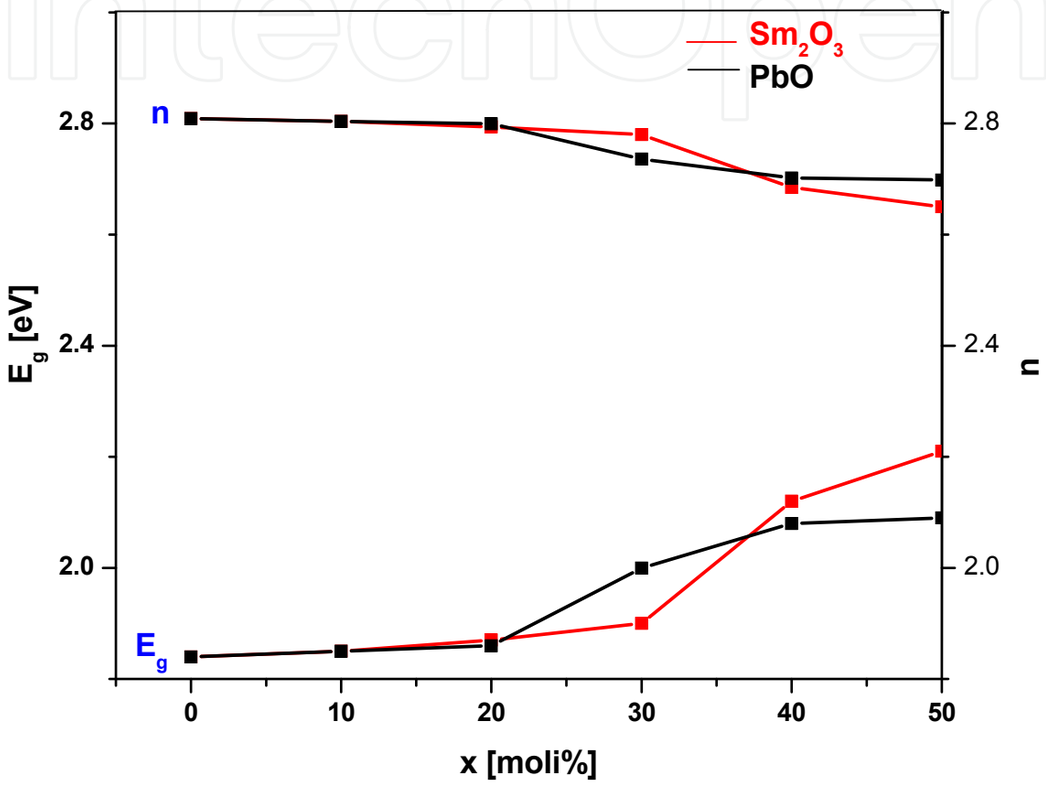

Fig. 6. The relationship between the optic gap, E_g, and refractive index, n, and the and the PbO or Sm_2O_3 contents (the line is only a guide for the eye).

In brief, we can conclude that the optical band gap increases with increasing the PbO or Sm_2O_3 contentof the glass. Since the basic structural units of the vanadate-tellurate glasses are known to be the [TeO_3] and [VO_4] structural units and the internal vibrations of these molecular units take part in the transitions. In this work, the increase of the optical band gap, Eg, to larger energies with increasing the PbO or Sm_2O_3 content is probably related to the progressive decrease in the concentration of non-bridging oxygen. This decrease in turn gives rise to a possible decrease in the bridging Te-O-Te and V-O-V linkages. The shift is attributed to structural changes which are the the result of the different (interstitial or substitutional) site occupations of the Pb^{+2} or Sm^{+3} ions which are added to the vanadate-tellurate matrix and modify the network.

We assume that as the cation concentration increases, the Te-O-Te and V-O-V linkages develop bonds with Pb^{+2} or Sm^{+3} ions, which in turn leads to the gradual breakdown of the

glass network. This effect seems more pronounced in doping of the network with the Sm^{+3} ions. These results are in agreement with XRD data which indicate the higher affinity of the samarium ions to attract structural units with negative charge yielding the formation of the $SmVO_4$ crystalline phase for samples with x>30mol%.

3.3 DFT calculations

In this section, the purpose of the present paper was to continue the investigation of the structure of the vanadate-tellurate network and especially to illuminate structural aspects of the vanadate network using quantum-chemical calculations because the coordination state of vanadium atoms is not well understood. Figure 7 shows the optimized structure proposed to the $3TeO_2 \cdot 2V_2O_5$ glass network.

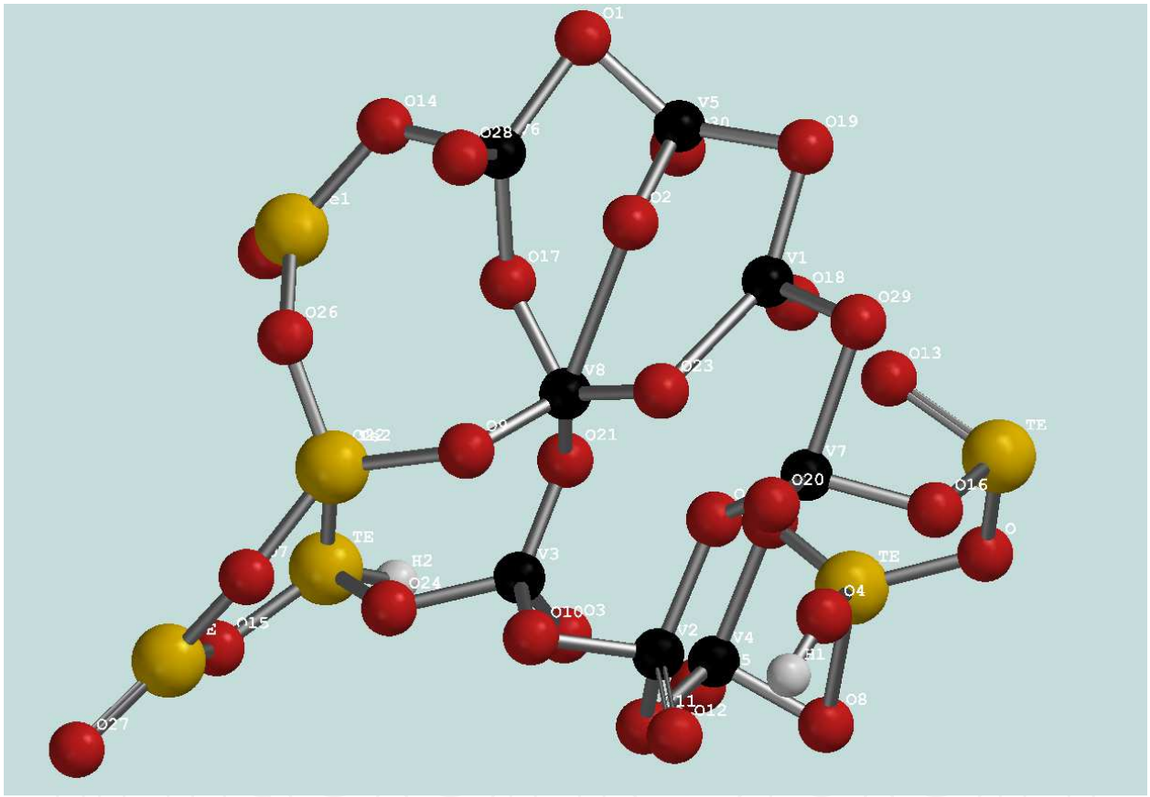

Fig. 7. Optimized structure of the model for binary $3TeO_2 \cdot 2V_2O_5$ glassy.

Analyzing the structural changes resulted from the geometry optimization of our model, we found that the vanadium ions are distributed into two crystallographic sites: the $[VO_4]$ tetrahedral and $[VO_5]$ square pyramidal units. The vanadium tetrahedrons are very regular with vanadium-oxygen distances ranging from 1.57 to 1.82Å and O-V-O angles ranging from 104^0 to 110^0 (with a mean value (109.5^0) very close to the ideal value (109.28^0) corresponding to the tetrahedral geometry). In our model, the V-O interatomic bond distances are ranging from 1.60 to 1.65Å, 1.75 to 1.80Å (the average V-O distance is 1.72Å) and O-V-O angles values are ranging from 101 to 112^0. This result show that the $[VO_4]$ tetrahedrons are easy distorted around the vanadium center.

The [VO_5] square pyramidal units are considerably distorted around the vanadium center and the V-O bond distances are ranging from 1.65 to 2.30Å. Such a behavior was reported for the two-dimensional layered vanadate compounds [35, 36]. This shows that there is instability in the nonequivalent V-O bonds in the polyhedron. In essence, this is due to the displacement of the vanadium atom from the centre of the polyhedron, whose asymmetry strongly depends on the manner of connection with the surrounding polyhedron. This deformation will be expressed more clearly in the formation of the vitreous matrix.

This structural model shows a very complex behavior of the vanadium atoms and their stabilization can be achieved by the formation of orthovanadate structural units or by the intercalation of [PbO_3] structural units in the immediate vicinity of these units.

4. Conclusions

The X-ray diffraction patterns reveal the $SmVO_4$ crystalline phase in the samples with x>30mol% Sm_2O_3 indicating that the samarium ions have an pronounced affinity towards the vanadate structural units. By adding of Sm_2O_3 content in the host matrix, the FTIR spectra suggests that the glass network modification has taken place mainly in the vanadate part whereas by adding of PbO, the network is transformed from a vanadate-tellurate network into a continuous lead-vanadate-tellurate network by Te-O-Pb and V-O-Pb linkages.

The UV-VIS absorption spectra of the studied samples reveal the additional absorptions in the 250-1050nm range due to the generation of $n \rightarrow \pi^*$ transitions and the presence of the transition or rare earth metallic ions. By increasing the metal oxide content up to 50mol%, the optical band gap energy increases. This suggests a decrease of the non-bridging oxygens due to the formation of orthovanadate (for adding Sm_2O_3) and [PbO_3] (for adding PbO) structural units, respectively. The band gap energy was changed due to structural modifications of the network.

Our DFT investigations show that the penta-coordinated vanadium atoms show a unique influence on the structural properties of the glasses.

5. Acknowledgments

The financial support of the Ministry of Education and Research of Romania-National University Research Council (CNCSIS, PN II-IDEI 183/2008, contract number 476/2009) is gratefully acknowledged by the authors.

6. References

[1] S. Tanaba, K. Hirao, N. Soga, J. Non-Cryst. Solids 122 (1990) 79.
[2] H. Nasu, O. Matsusita, K. Kamiya, H. Kobayashi, K. Kubodera, J. Non-Cryst. Solids 124 (1990) 275.
[3] B. Eraiah, Bull. Mater. Sci. 29(4) (2006) 375.
[4] G. Nunziconti, S. Bemeschi, M. Bettinelli, M. Brei, B. Chen, S. Pelli, A. Speghini, G. C. Righini, J. Non-Cryst. Solids 345&346 (2004) 343.
[5] M. Ganguli, M. Bhat Harish, K. J. Rao, Phys. Chem. Glasses 40 (1999) 297.

[6] S. Jayaseelan, P. Muralidharan, M. Venkateswarlu, N. Satyanarayana, Mater. Chem. Phys. 87 (2004) 370.
[7] G. A. Kumar, A. Martinez, A. Mejia, C. G. Eden, J. Alloys Compd. 365 (2004) 117.
[8] J. Yang, S. Dai, Y. Zhou, L. Wen, L. Hu, Z. H. Jiang, J. Appl. Phys. 93 (2003) 977.
[9] W. A. Pisarski, T. Goryczka, B. Wodecka-Dus, M. Plonska, J. Pisarska, Mater. Sci. Eng. 122 (2005) 94.
[10] G. Lakshminarayana, S. Buddhudu, Mater. Chem. Phys. 102 (2007) 181.
[11] Thulasiramudu, S. Buddhudu, Spectrochim Acta A 67 (2007) 802.
[12] Spartan'04, Wavefunction Inc., 18401 Von Karman Avenue, Suite 370 Irvine, CA 92612.
[13] M. J. Frisch, G. W. Trucks, H. B. Schlegel, G. E. Scuseria, M. A. Robb, J. R. Cheeseman, J. A. Montgomery, Jr., T. Vreven, K. N. Kudin, J. C. Burant, J. M. Millam, S. S. Iyengar, J. Tomasi, V. Barone, B. Mennucci, M. Cossi, G. Scalmani, N. Rega, G. A. Petersson, H. Nakatsuji, M. Hada, M. Ehara, K. Toyota, R. Fukuda, J. Hasegawa, M. Ishida, T. Nakajima, Y. Honda, O. Kitao, H. Nakai, M. Klene, X. Li, J. E. Knox, H. P. Hratchian, J. B. Cross, C. Adamo, J. Jaramillo, R. Gomperts, R. E. Stratmann, O. Yazyev, A. J. Austin, R. Cammi, C. Pomelli, J. W. Ochterski, P. Y. Ayala, K. Morokuma, G. A. Voth, P. Salvador, J. J. Dannenberg, V. G. Zakrzewski, S. Dapprich, A. D. Daniels, M. C. Strain, O. Farkas, D. K. Malick, A. D. Rabuck, K. Raghavachari, J. B. Foresman, J. V. Ortiz, Q. Cui, A. G. Baboul, S. Clifford, J. Cioslowski, B. B. Stefanov, G. Liu, A. Liashenko, P. Piskorz, I. Komaromi, R. L. Martin, D. J. Fox, T. Keith, M. A. Al-Laham, C. Y. Peng, A. Nanayakkara, M. Challacombe, P. M. W. Gill, B. Johnson, W. Chen, M. W. Wong, C. Gonzalez, and J. A. Pople, Gaussian 03, Revision A.1, Gaussian, Inc., Pittsburgh PA, 2003.
[14] S. Rada, M. Culea, E. Culea, J. Phys. Chem. A 112(44) (2008) 11251.
[15] S. Rada, M. Neumann, E. Culea, Solid State Ionics 181 (2010) 1164.
[16] S. Rada, E. Culea, M. Rada, Mater. Chem. Phys. 128(3) (2011) 464.
[17] S. Rada, E. Culea, M. Culea, Borate-Tellurate Glasses: An Alternative of Immobilization of the Hazardous Wastes, Nova Science Publishers INC., New York, 2010.
[18] S. Rada, E. Culea, J. Molec. Struct. 929 (2009) 141.
[19] M. Rada, V. Maties, S. Rada, E. Culea, J. Non-Cryst. Solids 356 (2010) 1267.
[20] S. Rada, R. Chelcea, E. Culea, J. Molec. Model. 17 (2011) 165.
[21] S. Rada, E. Culea, M. Culea, J. Mater. Sci. 43(19) (2008) 6480.
[22] K. V. Ramesh, D. L. Sastry, J. Non-Cryst. Solids 352 (2006) 5421.
[23] K. Gatterer, G. Pucker, H. P. Fritzer, Phys. Chem. Glasses 38 (1997) 293.
[24] S. Rada, M. Culea, E. Culea, J. Non-Cryst. Solids 354(52-54) (2008) 5491.
[25] S. Rada, M. Culea, M. Neumann, E. Culea, Chem. Phys. Letters 460 (2008) 196.
[26] M. Rada, V. Maties, M. Culea, S. Rada, E. Culea, Spectrochim. Acta A 75 (2010) 507.
[27] M. T. Abd El-Ati, A. A. Higazy, J. Mater. Sci. 35 (2000) 6175.
[28] S. N. Misra, S. O. Sommerer, Appl. Spectrosc. Rev. 26 (1991) 151.
[29] V. K. Tikhomirov, M. Naftaly, A. Jha, J. Appl. Phys. 86 (1999) 351.
[30] D. Ehrt, J. Non-Cryst. Solids 348 (2004) 22.
[31] A. M. Nassar, N. A. Ghoneim, J. Non-Cryst. Solids 46 (1981) 181.
[32] T. Aoki, Y. Hatanaka, D.C. Look, Appl. Phys. Lett. 76 (2000) 3257.
[33] W. R. Salaneck, C. R. Wu, J. L. Bredas, J. J. Ritsko, Chem. Phys. Lett. 127 (1986) 88.
[34] R. El-Mallawany, J. Appl. Phys. 72 (1992) 1774.

[35] Sun, E. Wang, D. Xiao, H. An, L. Xu, J. Molec. Struct. 840 (2007) 53.
[36] Y. Zhou, H. Qiao, Inorg. Chem. Comm. 10 (2007) 1318.

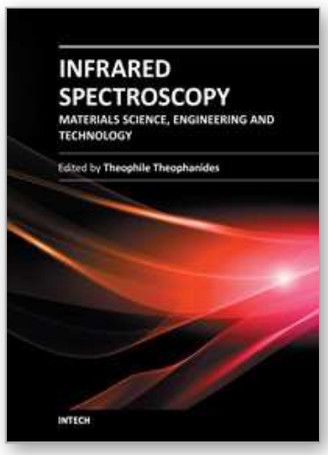

Infrared Spectroscopy - Materials Science, Engineering and Technology

Edited by Prof. Theophanides Theophile

ISBN 978-953-51-0537-4
Hard cover, 510 pages
Publisher InTech
Published online 25, April, 2012
Published in print edition April, 2012

The present book is a definitive review in the field of Infrared (IR) and Near Infrared (NIR) Spectroscopies, which are powerful, non invasive imaging techniques. This book brings together multidisciplinary chapters written by leading authorities in the area. The book provides a thorough overview of progress in the field of applications of IR and NIR spectroscopy in Materials Science, Engineering and Technology. Through a presentation of diverse applications, this book aims at bridging various disciplines and provides a platform for collaborations among scientists.

How to reference

In order to correctly reference this scholarly work, feel free to copy and paste the following:

E. Culea, S. Rada, M. Culea and M. Rada (2012). Structural and Optical Behavior of Vanadate-Tellurate Glasses Containing PbO or Sm2O3, Infrared Spectroscopy - Materials Science, Engineering and Technology, Prof. Theophanides Theophile (Ed.), ISBN: 978-953-51-0537-4, InTech, Available from: http://www.intechopen.com/books/infrared-spectroscopy-materials-science-engineering-and-technology/structural-and-optical-behavior-of-vanadate-tellurate-glasses

INTECH
open science | open minds

InTech Europe
University Campus STeP Ri
Slavka Krautzeka 83/A
51000 Rijeka, Croatia
Phone: +385 (51) 770 447
Fax: +385 (51) 686 166
www.intechopen.com

InTech China
Unit 405, Office Block, Hotel Equatorial Shanghai
No.65, Yan An Road (West), Shanghai, 200040, China
中国上海市延安西路65号上海国际贵都大饭店办公楼405单元
Phone: +86-21-62489820
Fax: +86-21-62489821

IntechOpen